

# Ceramides in peripheral arterial plaque lead to endothelial cell dysfunction

Rodrigo Meade, BS,<sup>a</sup> Yang Chao, MD, PhD,<sup>a</sup> Nikolai Harroun, MD,<sup>a</sup> Chenglong Li, MD,<sup>a</sup> Shahab Hafezi, MD,<sup>a</sup> Fong-Fu Hsu, PhD,<sup>b</sup> Clay F. Semenkovich, MD,<sup>b</sup> and Mohamed A. Zayed, MD, PhD, MBA,<sup>a,c,d,e,f</sup> St. Louis, MO

## ABSTRACT

**Background:** Peripheral arterial atheroprogession is increasingly prevalent, and is a risk factor for major limb amputations in individuals with risk factors such as diabetes. We previously demonstrated that bioactive lipids are significantly altered in arterial tissue of individuals with diabetes and advanced peripheral arterial disease.

**Methods:** Here we evaluated whether sphingolipid ceramide 18:1/16:0 (C16) is a cellular regulator in endothelial cells and peripheral tibial arterial tissue in individuals with diabetes.

**Results:** We observed that C16 is the single most elevated ceramide in peripheral arterial tissue from below the knee in individuals with diabetes (11% increase,  $P < .05$ ). C16 content in tibial arterial tissue positively correlates with sphingomyelin (SPM) content in patients with and without diabetes ( $r^2 = 0.5$ ,  $P < .005$ ;  $r^2 = 0.17$ ,  $P < .05$ ; respectively). Tibial arteries of individuals with diabetes demonstrated no difference in *CERS6* expression (encoding ceramide synthase 6; the predominate ceramide synthesis enzyme), but higher *SMPD* expression (encoding sphingomyelin phosphodiesterase that catalyzes ceramide synthesis from sphingomyelins;  $P < .05$ ). *SMPD4*, but not *SMPD2*, was particularly elevated in maximally diseased (Max) tibial arterial segments ( $P < .05$ ). In vitro, exogenous C16 caused endothelial cells (HUVECs) to have decreased proliferation ( $P < .03$ ), increased apoptosis ( $P < .003$ ), and decreased autophagy ( $P < .008$ ). Selective knockdown of *SMPD2* and *SMPD4* decreased native production of C16 ( $P < .01$  and  $P < .001$ , respectively), but only knockdown of *SMPD4* rescued cellular proliferation ( $P < .005$ ) following exogenous supplementation with C16.

**Conclusions:** Our findings suggest that C16 is a tissue biomarker for peripheral arterial disease severity in the setting of diabetes, and can impact endothelial cell viability and function.

**Clinical relevance:** Peripheral arterial disease and its end-stage manifestation known as chronic limb-threatening ischemia (CLTI) represent ongoing prevalent and intricate medical challenges. Individuals with diabetes have a heightened risk of developing CLTI and experiencing its complications, including wounds, ulcers, and major amputations. In the present study, we conducted a comprehensive examination of the molecular lipid composition within arterial segments from individuals with CLTI, and with and without diabetes. Our investigations unveiled a striking revelation: the sphingolipid ceramide 18:1/16:0 emerged as the predominant ceramide species that was significantly elevated in the peripheral arterial intima below the knee in patients with diabetes. Moreover, this heightened ceramide presence is associated with a marked impairment of endothelial cell function and viability. Additionally, our study revealed a concurrent elevation in the expression of sphingomyelin phosphodiesterases, enzymes responsible for catalyzing ceramide synthesis from sphingomyelins, within maximally diseased arterial segments. These findings underscore the pivotal role of ceramides and their biosynthesis enzymes in the context of CLTI, offering new insights into potential therapeutic avenues for managing this challenging disease process. (*JVS—Vascular Science* 2023;4:100181.)

**Keywords:** Ceramide; Diabetes; Endothelial dysfunction; Peripheral arterial disease; Sphingolipid; Sphingomyelinase

From the Section of Vascular Surgery, Department of Surgery,<sup>a</sup> Division of Endocrinology, Lipid, and Metabolism, Department of Internal Medicine,<sup>b</sup> Department of Radiology,<sup>d</sup> and Roy and Diana Vagelos Division of Molecular Cell Biology,<sup>e</sup> Washington University School of Medicine; the Department of Surgery, Veterans Affairs St. Louis Health Care System,<sup>c</sup> and the Department of Biomedical Engineering, McKelvey School of Engineering, Washington University.<sup>f</sup>

This work was supported by grants from the Vascular Cures Foundation Wylie Scholar Award (to M.A.Z.), American Surgical Association Research Fellowship Award (to M.A.Z.), Society for Vascular Surgery Foundation Research Investigator Award (to M.A.Z.), and Washington University School of Medicine Diabetes Research Center (National Institute of Diabetes and Digestive Kidney Disease, National Institutes of Health [NIH] grant P30 DK020589; National Heart, Lung, and Blood Institute [NHLBI], NIH grant K08 HL132060 to M.A.Z.; NHLBI, NIH grant R01 HL153262 to M.A.Z., NHLBI, NIH grant R01 HL150891 to M.A.Z., National Institute of Diabetes and Digestive Kidney Disease, NIH grant R01 DK101392 to C.F.S., and NIH, NHLBI grant R01 HL157154

to C.F.S.). The Washington University School of Medicine Mass Spectrometry Facility is supported by the U.S. Public Health Service (grants P41-GM103422 and P60-DK-20579).

Correspondence: Mohamed A. Zayed, MD, PhD, MBA, DFSVS, FAHA, FACS, Section of Vascular Surgery, Department of Surgery, Washington University School of Medicine, Campus Box 8109 – Surgery, 660 S Euclid Ave, St. Louis, MO 63110-1093 (e-mail: [zayedm@wustl.edu](mailto:zayedm@wustl.edu)).

The editors and reviewers of this article have no relevant financial relationships to disclose per the Journal policy that requires reviewers to decline review of any manuscript for which they may have a conflict of interest.

2666-3503

Published by Elsevier Inc. on behalf of the Society for Vascular Surgery. This is an open access article under the CC BY-NC-ND license (<http://creativecommons.org/licenses/by-nc-nd/4.0/>).

<https://doi.org/10.1016/j.jvssci.2023.100181>

Peripheral arterial disease (PAD) is, for the most part, a consequence of longitudinal development of atherosclerotic plaque in the peripheral arterial system.<sup>1,2</sup> This chronic disease affects >200 million adults worldwide, and its management consumes >\$300 billion in health care costs annually.<sup>3–6</sup> Diabetes is a major risk factor for peripheral arterial atheroprotection that afflicts the below the knee tibial arteries in particular, increases the prevalence of PAD-associated complications such as chronic limb-threatening ischemia (CLTI), and increases the incidence of major lower extremity amputations.<sup>7–9</sup> Understanding the underlying biochemical mechanisms that influence atheroprotection in the peripheral arterial system of individuals with diabetes is essential for improving therapeutic effectiveness and the prevention of PAD-related complications.<sup>2</sup>

It is known that tissue lipids are important mediators of atheroprotection and affect endothelial cell (EC) function and health.<sup>10</sup> However, a paucity of studies have evaluated how bioactive lipids in arterial tissue can affect the incidence and severity of PAD progression—in particular, in the tibial arteries and in the setting of diabetes.<sup>11</sup> Previous studies suggest that ceramides and bioactive sphingolipids that are essential for cellular membrane homeostasis play important roles in maintaining vascular tissue structural integrity and function and can influence atherosclerotic plaque formation.<sup>12–18</sup> However, the direct effects of specific ceramide species on atheroprotection are not well understood.

De novo biosynthesis of ceramides in the liver and other organs occurs via condensation of various fatty acetyl-coenzyme A molecules with sphingoid bases, including dihydrosphingosine. This biochemical reaction is catalyzed by different isoforms of ceramide synthases.<sup>19</sup> However, ceramides can also be synthesized through alternative biochemical pathways, including from sphingosines via the endolysosomal system and from the hydrolysis of sphingomyelins (SPMs) via sphingomyelinases.<sup>20</sup> It remains unknown which, if any, of these major ceramide synthesis pathways occur in peripheral arterial tissue, affect autocrine and paracrine cellular signaling in arterial tissue, and influence cellular signaling cascades that contribute to atherosclerosis in the peripheral arterial system.

We evaluated the content of ceramides in the lower leg tibial arteries of the peripheral arterial system of individuals with and without diabetes with advanced, nonsalvageable CLTI. We also evaluated which ceramide synthesis mechanisms influence EC viability and function. We hypothesized that in the setting of diabetes, unique ceramide species and synthesis pathways could play important roles in EC viability and function.

## METHODS

### Human peripheral vascular tissue procurement

Individuals with severe lower leg ischemia (Rutherford class 5 and 6) and nonsalvageable CLTI (both medical

and surgical revascularization failed), who were undergoing major lower extremity amputations, were prospectively enrolled into an institutional review board-approved vascular tissue biobank. All participants provided written informed consent before inclusion in the present study. Immediately after lower extremity amputation in the operating room, diseased and/or occluded tibial artery segments that had not undergone prior arterial intervention (ie, atherectomy, angioplasty, and/or stenting) and were in the lower leg regions with no gross infection were harvested en bloc, placed in cold saline solution, and transported immediately on ice to the laboratory for isolation of the arterial intima, as previously described.<sup>1</sup> For all specimens, the arterial intima was subdivided into maximally diseased and minimally diseased segments, as previously described.<sup>1</sup> Arterial intima segments were either embedded in paraffin, snap frozen in liquid nitrogen and stored at  $-80^{\circ}\text{C}$  for subsequent analysis or preserved for RNA isolation. Patient demographics, including age, medical comorbidities, and medications, were also recorded (Table).

### Arterial tissue protein analysis

Arterial tissue segments were immersed in cold hypotonic nondetergent-based lysis buffer (1 M  $\text{NaHCO}_3$ , 1 M sucrose, 1.5 M  $\text{NaN}_3$ , 0.1 M phenylmethylsulfonyl fluoride, and Protease Inhibitor Cocktail Set III; Calbiochem) for 30 minutes. Tissue was lysed in cold lysis buffer (0.01 M  $\text{NaHCO}_3$ , 250 mM sucrose, 5 mM  $\text{NaN}_3$ , and 0.1 mM phenylmethylsulfonyl fluoride). All specimens were then homogenized with a high-speed rotational power tissue homogenizer (Glas-Col LLC). Homogenized samples underwent centrifugation at 4697g for 5 minutes, and the supernatants were obtained to standardize the protein concentration using a colorimetric Bradford protein concentration assay (Bio-Rad).

### EC in vitro assays

Primary human umbilical vein endothelial cells (HUVECs; passages 4–6) were cultured on 1% gelatin-coated culture plates using EC growth medium-2 supplemented with 10% fetal bovine serum, 1% antibiotics (100 U/mL of penicillin, 100  $\mu\text{g}/\text{mL}$  of streptomycin), vascular endothelial growth factor (1 ng/mL), basic fibroblast growth factor (2 ng/mL), and heparin (10 U/mL). HUVECs were treated with C2 ceramide (10  $\mu\text{M}$ ; model no. A7191; Sigma-Aldrich), sphingolipid ceramide 18:1/16:0(C16; 10  $\mu\text{M}$ ; model no. 860516p; Sigma-Aldrich) or ethanol (2  $\mu\text{M}$ ) in basal media for 6 hours. Ceramides were dissolved into 100% chloroform for a solution concentration of 10 mM and dried with nitrogen gas. The ceramides were reconstituted in phosphate-buffered saline to 100  $\mu\text{M}$  and sonicated until fully dissolved. Ceramide were then added to ECs in in vitro cultures at 1:10 dilution for 10  $\mu\text{M}$ . The ECs were then lysed in

**Table.** Patient cohort demographics<sup>a</sup>

Variable	Diabetes mellitus		P value
	No (n = 7)	Yes (n = 14)	
Age, years	63.7 ± 13.73	65.7 ± 8.6	.73
Gender			.37
Male	4	7	
Female	3	5	
BMI, kg/m <sup>2</sup>	25.8 ± 6.3	27.2 ± 5.7	.63
Current smoker	2	5	.36
Hypertension	6	13	.47
Hyperlipidemia	4	9	.34
Coronary artery disease	2	6	.31
End-stage renal disease	1	4	.01
Statin therapy	3	7	.34
Insulin therapy	0	7	.03
HbA1c, %	NA	7.9 ± 1.6	NA

BMI, Body mass index; HbA1c, hemoglobin A1c; NA, not applicable.

<sup>a</sup>Patients with (n = 14) and without (n = 7) diabetes who underwent lower extremity amputations were enrolled in the Washington University Vascular Tissue BioBank; their demographics were retrospectively reviewed and evaluated in the two study groups. With the exception of insulin therapy, none of the other variables were significantly different between the patient groups.

radioimmunoprecipitation assay buffer and stored at −80°C. Lysate concentrations were determined using a Bradford protein analysis assay (Bio-Rad).

### Western blotting

Aliquots of 20 μg of homogenates of human arterial intima segments, primary ECs, and cells from the MCF7 breast cancer cell line (control) were separated on a 4% to 20% gradient sodium dodecyl sulfate-tris-glycine-polyacrylamide gel and electro-transferred onto polyvinylidene difluoride membranes. The membranes were blocked with 5% bovine serum albumin and then probed overnight with LC-3 (Novus Biologicals) and glyceraldehyde 3-phosphate dehydrogenase antibodies (Cell Signaling Technologies). The LC-3 ratio was measured by dividing the content of the activated LC-3 II isoform by the cytoplasmic LC-3 I isoform as quantified by the densitometry of the bands on Western blots. The membranes were then incubated for 2 hours with a horseradish peroxidase anti-rabbit secondary antibody and resolved with an ECL kit (Thermo Fisher Scientific) and LI-COR imaging system. Band densitometry analysis was performed using ImageJ software, as previously described. Band densities were averaged across triplicate blots and are expressed as ratios relative to protein loading control or nonphosphorylated total protein.

### Mass spectrometry ceramide content analysis

The mass spectrometry-derived lipid mass spectrum for each sample was averaged over time, and the average background spectra were subtracted, as previously described.<sup>1,21</sup> The ceramide content was determined

using a custom algorithm in MATLAB (MathWorks, Inc). The absolute lipid concentration was obtained by deriving the ratio of the signal intensity of each ceramide species against the known quantity of the homologous, non-naturally occurring internal standard. This analysis included 11 SPMs and seven ceramide lipid species.

### Lipid extraction and lipidomic assay

At 24 hours after transfection with small interfering RNA (siRNA), HUVECs were lysed and lipids isolated for lipidomic analysis, as previously described.<sup>21</sup> Supernatant aliquots were obtained for each sample, and a set quantity of homologous non-naturally occurring phospholipid internal standard species was added to each aliquot. The internal standard cocktail included 1,2-dimyristoyl-sn-glycero-3-phosphocholine (phosphatidylcholine ratio, 14:0/14:0), dimyristoyl-sn-glycero-3-phosphoethanolamine (ratio, 14:0/14:0), dimyristoyl-sn-glycero-3-phosphoserine (phosphatidylserine ratio, 14:0/14:0), dimyristoyl-sn-glycero-3-phosphoglycerol (phosphatidylglycerol ratio, 14:0/14:0), dipalmitoyl-sn-glycero-3-phosphoinositol (phosphatidylinositol ratio, 16:0/16:0), and N-lauroyl-D-erythro-sphingosine (ceramide ratio, d18:1/12:0). Samples were then extracted by adding chloroform–methanol (2:1), 0.63 LiCl solution, and chloroform in sequence and centrifuging. The organic phase from two extractions (twice) was pooled and dried under nitrogen gas. Lipids were dissolved in 1% ammonium hydroxide in methanol before analysis. Lipid extracts from transfected HUVECs were analyzed by direct injection electrospray ionization mass spectrometry using a Vantage triple-quadrupole mass spectrometer (Thermo Fisher Scientific) and an Accela 1250 UPLC system (Thermo Fisher Scientific) operated via the Xcalibur operating

system (Thermo Fisher Scientific). Structures for all phospholipids were identified using methods previously described.<sup>21</sup>

### Real-time polymerase chain reaction

Real-time polymerase chain reaction (PCR) RNA was performed in HUVECs, mouse lung ECs, and human arterial intima tissue, as previously described.<sup>1</sup> The extracted RNA mixture was amplified using Applied Biosystems PowerUp SYBR Green Master Mix (model no. A25742; Thermo Fisher Scientific). Samples were evaluated using the 7500 Fast Real-Time PCR System (Applied Biosystems, Thermo Fisher Scientific). mRNA primers (Supplementary Table I) were used to evaluate the relative expression of *RPL32* (housekeeping gene), SMP phosphodiesterase 2 (*SMPD2*), and SPM phosphodiesterase 4 (*SMPD4*). Values were calculated using the  $2^{-\Delta\Delta CT}$  method and normalized relative to the abundance of *RPL32*.<sup>22</sup>

**Cell lines, chemicals, and biochemicals.** HUVECs were purchased from ATCC (model no. PCS-100-013). Ceramides C2 and C16 were obtained from Avanti Polar Lipids. The BrdU (bromodeoxyuridine) cell proliferation enzyme-linked immunosorbent assay (ELISA) kit (model no. ab126556) was purchased from Abcam. The cell death detection ELISA plus kit was obtained from Sigma-Aldrich. The MCF7 breast cancer cell line was purchased from ATCC (model no. HTB-22).

### SMPD siRNA

siRNAs (*siSMPD2* AM16708 and *siSMPD4* AM16790; Thermo Fisher Scientific) and a negative control (enhanced green fluorescent protein) were purchased from Applied Biosystems. Transfection of siRNAs into HUVECs was performed using Lipofectamine RNAiMAX (Thermo Fisher Scientific) in accordance with the manufacturer's instructions. The siRNAs were used at a final concentration of 10 nM. Quantitative real-time PCR was performed at 24 hours after transfection. Transfection efficiency was monitored by transfection of KIF11 (Thermo Fisher Scientific).

### Cell proliferation assay

Cell proliferation and death were evaluated using a BrdU incorporation assay and anti-DNA/histone ELISA, respectively. In a 96-well culture format,  $1 \times 10^4$  ECs were seeded per well, followed by serum starvation for  $\geq 6$  hours. Corresponding treatment of growth media, vehicle, C2, and C16 was independently evaluated after 24 hours in accordance with the manufacturer's instructions (Roche) using a multiwell spectrophotometer at 450 nm, as previously described.<sup>23,24</sup> Each assay was repeated in triplicate.

### Statistical analysis

All statistical analyses were performed using GraphPad Prism. Lipidomic comparisons were evaluated using the

two-way Student *t* test. Comparisons between individual HUVEC treatment conditions were evaluated using two-way analysis of variance and unpaired two-way Student *t* test. Similarly, ELISA assays were evaluated using two-way analysis of variance. Values of  $P < .05$  were considered statistically significant. Descriptive statistics are summarized as the mean  $\pm$  standard error of the mean, unless stated otherwise.

## RESULTS

**Peripheral arterial lipid content.** We comprehensively evaluated the lipid content in arterial segments of 21 patients who underwent a major lower extremity amputation due to nonsalvageable CLTI. Patients with ( $n = 14$ ) and without ( $n = 7$ ) diabetes were included in this study and had a similar age, demographics, and comorbidities (Table). Compared with patients without diabetes, the total content of lipid molecules was lower in the arterial intima segments of the patients with diabetes (Supplementary Table II;  $P = .039$ ). However, the relative content of ceramides and SPMs was higher (81.7% and 19.9%, respectively). Relative to the minimally diseased arterial intima, the total ceramide and SPM content was elevated in the maximally diseased segments of patients with diabetes (17.5% and 36.3%, respectively; Supplementary Table III) and in patients without diabetes (139.5% and 76.9%, respectively;  $P = .03$ ; Supplementary Table III).

Moreover, we observed a significant correlation between the total content of ceramides and SPM in tibial arterial intima of patients with and without diabetes (with diabetes:  $R^2 = 0.51$ ,  $P = .03$ , Fig 1, A; without diabetes:  $R^2 = 0.52$ ,  $P = .001$ , Fig 1, B). However, only in patients with diabetes did we observe that both minimally and maximally diseased arterial intima had a significant correlation between total ceramide and SPM (minimally:  $R^2 = 0.53$ ,  $P = .004$ ; maximally:  $R^2 = 0.47$ ,  $P = .006$ ; respectively; Fig 1, B).

### Ceramide and SPM in peripheral arterial segments.

Because ceramide and SPM lipid molecules were elevated in maximally diseased arterial segments, we further evaluated the content of individual lipid species. Among SPMs, SPM 34:1/1:0 (SPM34) was the most abundant SPM in the tibial arterial intima segments of patients with or without diabetes (Fig 1, C; Supplementary Fig 1). Among ceramides, we observed that C16 was the single most abundant lipid molecule in the peripheral arterial intima (Fig 1, D; Supplementary Fig 1). C16 was significantly higher in the arterial intima of patients with diabetes ( $P < .05$ ; Fig 1, E). C16 was also higher in the maximally diseased segments of patients with diabetes (101.1% higher;  $P = .04$ ) and without diabetes (323.8%;  $P = .02$ ; Fig 1, E; Supplementary Table II). Compared with the patients without diabetes (diabetes clinical severity index [DCSI], 0;  $n = 4$ ) and patients with a DCSI of  $\leq 5$  ( $n = 5$ ),

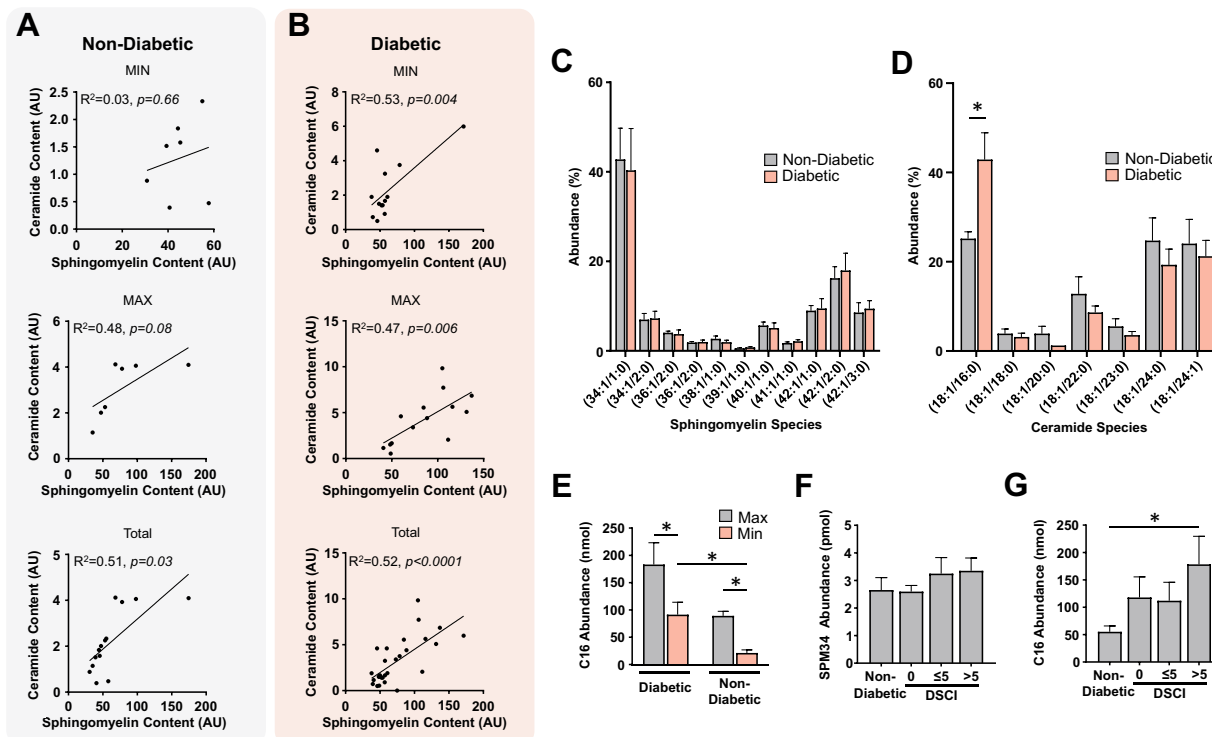


**Fig 1.** Ceramide 18:1/16:0 (C16) is elevated in diseased peripheral arterial intima. **A,B,** Lipidomic correlation of total ceramide and total sphingomyelin (SPM) content in minimally diseased tissue (*MIN*), maximally diseased tissue (*MAX*), and cumulatively (total) in arterial segments from patients without diabetes ( $n = 7$ ) and with diabetes ( $n = 14$ ). **C,** Total SPM abundance in diseased arterial segments separated by acetyl chain length ( $n = 10$ ). **D,** Total ceramide abundance of diseased arterial segments separated by acetyl chain length ( $n = 28$ ). **E,** C16 content in minimally and maximally arterial segments from patients without and with diabetes ( $n = 28$ ;  $P < .05$ ). **F,** Sphingomyelin 34:1/1:0 (SPM42) abundance stratified by diabetes complication severity index (DCSI) category ( $n = 14$ ). **G,** C16 abundance correlated with DCSI category ( $n = 28$ ).

patients with an elevated DCSI  $>5$  ( $n = 5$ ; indicative of higher diabetes-related clinical complications) demonstrated no observable differences in SPM34 (Fig 1, F) but higher C16 content in the maximally diseased arterial intima segments ( $P = .006$ ; Fig 1, G).

**Ceramide synthesis enzyme analysis.** To evaluate the synthetic pathways that might contribute to elevated C16 in diseased peripheral arterial intima, we examined the expression profiles of major catalytic enzymes responsible for ceramide synthesis. Expression of ceramide synthase 6 (encoded by *CERS6*) was similar in those with and without diabetes and in maximally and minimally diseased tibial arterial intima (Fig 2, A-C).

A significant correlation was found between total C16 and SPM34 molecules in those with diabetes ( $R^2 = 0.27$ ,  $P = .004$ ; Fig 2, D) and without diabetes ( $R^2 = 0.31$ ,  $P = .03$ ; Fig 2, E). Therefore, we evaluated whether *SMPDs*, which catalyze ceramide synthesis from SPMs via the alterative pathway, were differentially expressed in the peripheral arterial intima. Although no difference in expression was observed in isoforms *SMPD1* and *SMPD3* between patients with and without diabetes (Supplementary Fig 2, A and B), *SMPD2* was elevated in

patients without diabetes ( $P < .05$ ; Fig 2, F), and *SMPD4* was notably elevated in maximally diseased arterial intima segments ( $P < .05$ ; Fig 2, G). Although *SMPD1* was modestly elevated in maximally diseased segments (Supplementary Fig 2, C), *SMPD3* and *SMPD4* were overall higher in both patients with and without diabetes (Fig 2, H; Supplementary Fig 2, B). These findings suggest that upregulation of C16 in tibial arterial tissue might, in part, be regulated by *SMPD2* and *SMPD4* via the alterative synthesis pathway.

**Impact of C16 on EC viability and function.** EC dysfunction is a hallmark of atheroprogession and is a known contributor to PAD severity in the setting of diabetes.<sup>25</sup> We, therefore, evaluated whether supplementing ECs with exogenous C16 could affect EC function and viability. HUVECs maintained in culture at increasing concentrations of C16 or C18:1/2:0 (C2; as control), in particular with 12.5  $\mu\text{M}$  of C16, demonstrated a significant decrease in cellular proliferation (Fig 3, A). In addition, treatment of HUVECs with C16 was associated with a 40% increase in apoptosis, as visualized with caspase 3/7 immunostaining (Fig 3, B and C). Because cellular autophagy is a protective mechanisms that limits EC



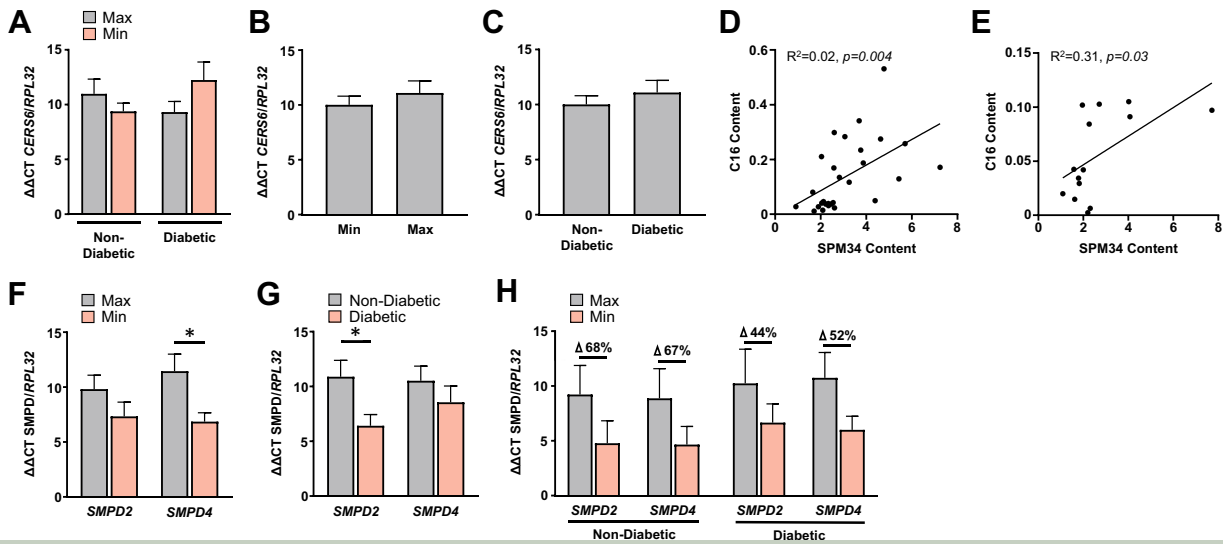


**Fig 2.** Expression profiles of ceramide synthesis enzymes in human tibial arterial tissue. **A**, Real-time (RT) polymerase chain reaction (PCR) of *CERS6* ratio with the *RPL32* housekeeping gene in the maximally (n = 5) and minimally (n = 4) diseased tissue of patients without diabetes vs maximally (n = 7) and minimally (n = 6) diseased tissue of patients with diabetes. **B**, RT-PCR of *CERS6* of total minimally (n = 10) and maximally (n = 12) diseased arterial intima segments. **C**, RT-PCR of *CERS6* in patients without diabetes (n = 9) and with diabetes (n = 13). **D**, Correlation of ceramide 18:1/16:0 (C16) and sphingomyelin 34:1/1:0 (SPM34) content in arterial intima segments of patients without diabetes (n = 14). **E**, Correlation of C16 and SPM34 in arterial intima segments of patients with diabetes (n = 28). **F**, RT-PCR of genes encoding for sphingomyelin phosphodiesterase enzymes 2 and 4 (*SMPD2* and *SMPD4*) and normalized to *RPL32*. This was evaluated in maximally (n = 5) and minimally (n = 4) arterial intima segments of patients without diabetes and maximally (n = 7) and minimally (n = 6) arterial intima segments from patients with diabetes. **G**, *SMPD2* and *SMPD4* normalized to *RPL32* in patients without diabetes (n = 9) and patients with diabetes (n = 13). **H**, *SMPD2* and *SMPD4* normalized to *RPL32* of maximally (n = 12) and minimally (n = 10) in patients with and without diabetes.

dysfunction,<sup>26,27</sup> we evaluated this process in the setting of exogenous C16 supplementation. We observed a 50% decrease in the activation of microtubule-associated proteins 1A/1B light chain 3B (LC3-II;  $P < .005$ ; Fig 3, D and E) in HUVECs supplemented with C16, suggesting that C16 inhibits protective cellular autophagy.

**Effect of *SMPD* on EC sensitivity to C16.** Because *SMPDs* can catalyze the synthesis of endogenous ceramides such as C16, and common isoforms were differentially expressed in diseased tibial arterial intima (Fig 2, F and H), we next evaluated whether selective knockdown of the *SMPD* genes can affect EC endogenous synthesis of C16 and cellular sensitivity to exogenous C16 supplementation.

Selective knockdown of either *SMPD2* or *SMPD4* in HUVECs with siRNA (*siSMPD2* and *siSMPD4*, respectively) was associated with a 20% decrease in endogenous C16 content ( $P = .001$ ; Fig 4, A). Protective cellular autophagy (LC-3 II/I ratio) was increased by >20% after knockdown of *SMPD2* and *SMPD4* in HUVECs that were exogenously supplemented with C2 (control, nonactive ceramide;  $P < .05$ ; Fig 4, B). However, C16 supplementation decreased autophagy in HUVECs with and without knockdown of *SMPD2* or *SMPD4* (Fig 4, B). This suggests that exogenous

C16 supplementation increases cellular stress conditions that deleteriously affect protective cellular autophagy and that *SMPD2* and *SMPD4* are essential for preserving autophagy and survival in HUVECs.<sup>26,27</sup>

To further investigate the impact of *SMPDs* on EC function, we evaluated the effect of exogenous C16 supplementation on HUVECs following knockdown of either *SMPD2* or *SMPD4*. Under control conditions with either solvent solution (without ceramides) or exogenous C2 supplementation, HUVEC proliferation was not affected (Fig 4, C). However, when HUVECs were stressed with exogenous C16 supplementation, only knockdown of *SMPD4* allowed HUVECs to have improved proliferation (Fig 4, C;  $P = .005$ ). These data suggest that inhibition of endogenous C16 synthesis by *SMPD4* knockdown can be protective in the setting of cellular stress imposed via exogenous C16 supplementation.

## DISCUSSION

Ceramides are well-recognized bioactive lipid molecules that play essential roles in cell membrane structure and integrity and regulation of various cell functions.<sup>25</sup> Regulation of ceramides is crucial for maintaining vascular homeostasis in the endothelium and known to contribute to cardiovascular disease progression.<sup>25,28,29</sup>

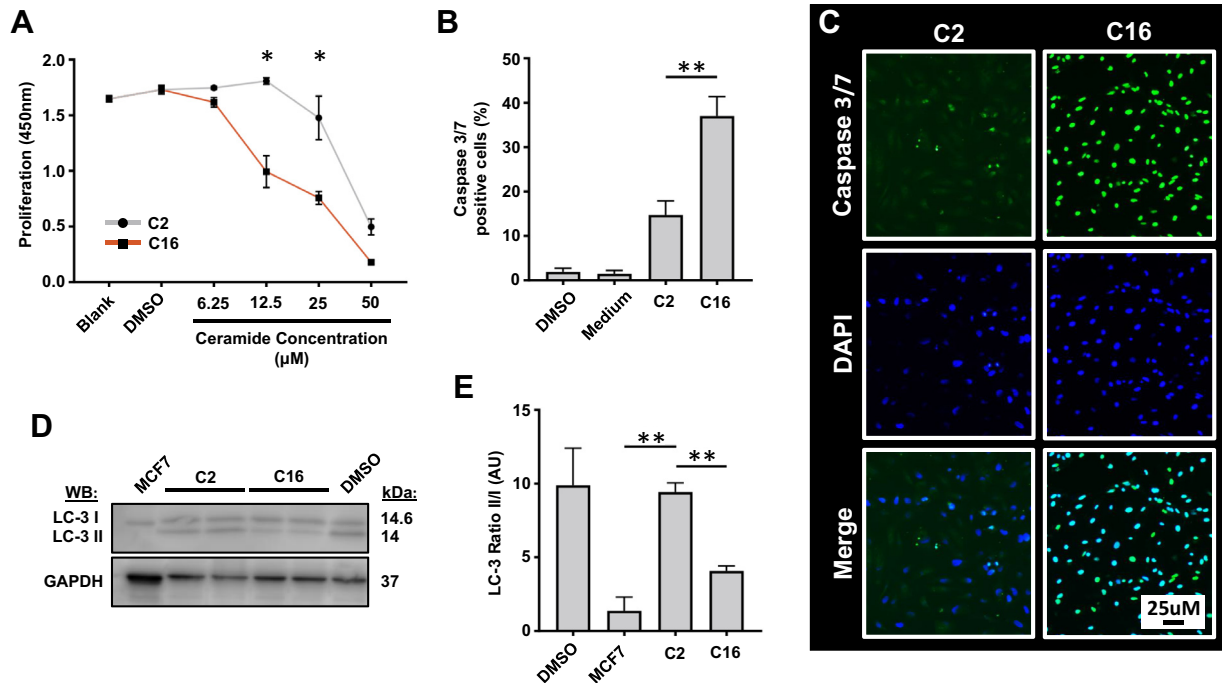


**Fig 3.** Ceramide 18:1/16:0 (C16) impairs human umbilical vein endothelial cell (HUVEC) viability and function. **A**, Proliferation of HUVEC cultures evaluated after treatment with C16 or C2 ( $P = .03$ ). **B,C**, HUVEC apoptosis analysis with caspase 3/7 immunostaining (CellEvent caspase-3/7 green detection reagent) compared with vehicle (ethanol) or solvent (ethanol in growth media). Relative to C2 controls, HUVECs treated with C16 demonstrated higher levels of apoptosis ( $P = .003$ ). **D**, Representative Western blot demonstrating decreased LC3II/I in HUVECs treated with C16. **E**, LC3II/I ratio is decreased in HUVECs treated with C16 ( $P = .008$ ). HUVECs treated with C2 demonstrated no significant differences in LC3II/I ratio relative to the positive vehicle control dimethyl sulfoxide (DMSO) and showed a significant difference relative to the negative control MCF7 breast cancer cell line ( $P = .006$ ).

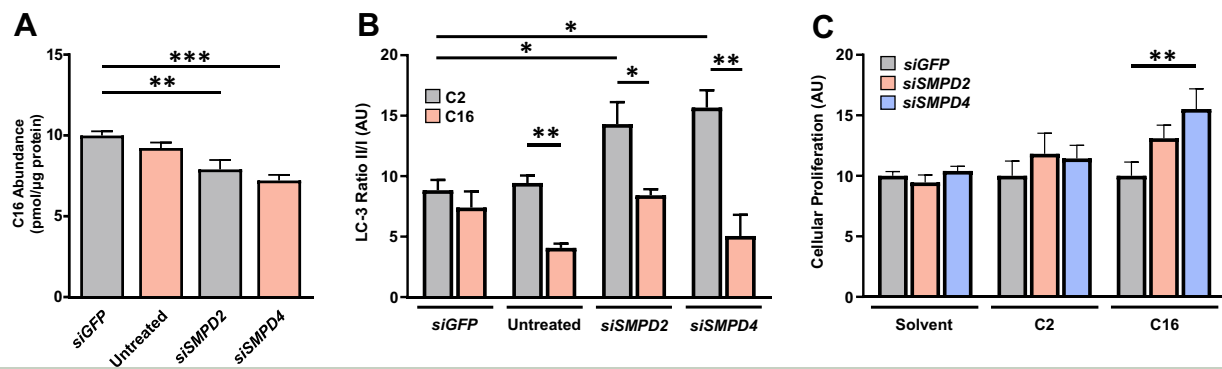


**Fig 4.** Effect of selective knockdown of sphingomyelin phosphodiesterases (SMPDs) in human umbilical vein endothelial cells (HUVECs). **A**, Small interfering RNA (siRNA) knockdown of *SMPD2* and *SMPD4* caused a decrease in ceramide 18:1/16:0 (C16) content in HUVECs compared with enhanced green fluorescent protein (GFP) siRNA control ( $P < .0001$ ,  $P = .006$ , and  $P < .0001$ , respectively). **B**, Selective knockdown of *SMPDs* in HUVECs followed by C2, C16, or vehicle (ethanol) supplementation. Each group is expressed relative to the vehicle treatment for each siRNA knockdown condition. Selective knockdown of *SMPD2* and *SMPD4* caused a decrease in LC3 ratio ( $P = .03$ ). **C**, Selective knockdown of *SMPD4* led to rescue of HUVEC proliferation after C16 treatment.

To the best of our knowledge, our study is the first to demonstrate that ceramide C16 is elevated in the peripheral tibial arterial intima of patients with CLTI. In vitro assessments demonstrated that C16 reduces EC

proliferation and viability and decreases protective cellular autophagy signaling. We also observed that ceramide production in diseased tibial arterial intima can be influenced by *SMPD*. Also, in nonstress conditions (in

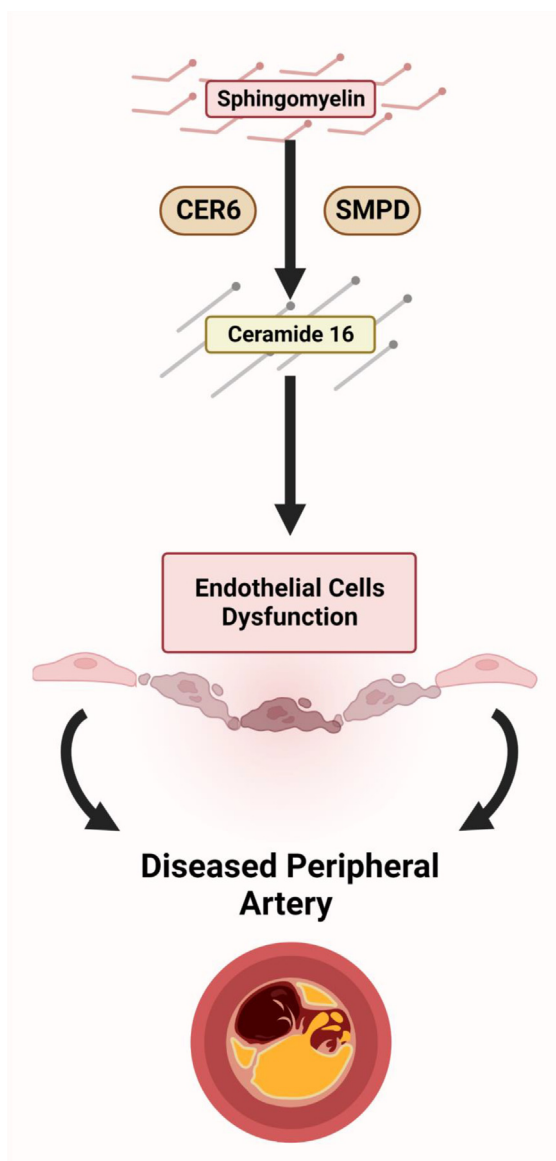


**Fig 5.** Ceramide 18:1/16:0 (C16) potentiates endothelial cell (EC) dysfunction and vascular disease. Sphingomyelin phosphodiesterases (SMPDs) can convert sphingomyelin substrate to ceramides such as C16. Increased peripheral arterial C16 leads to EC dysfunction, which ultimately contributes to atheroprotection and advanced forms of peripheral arterial disease (PAD) such as chronic limb-threatening ischemia (CLTI).

the absence of C16 supplementation), selective knock-down of *SMPDs* appeared to preserve EC autophagy and proliferation. These findings demonstrate that elevated C16 content in diseased tibial arterial intima could be a valuable tissue biomarker for disease severity and EC dysfunction (Fig 5).

Prior studies demonstrated that increased tissue ceramides can lead to decreased EC activation, disruption of mitochondrial electron transport chain, and increased reactive oxygen species production.<sup>30</sup> In

humans, circulating serum ceramides are elevated in individuals with obesity, diabetes, cancer, hepatic steatosis, hypertension, and coronary atherosclerosis.<sup>31</sup> In individuals with coronary artery disease, circulating ceramide levels are thought to be predictive of major adverse cardiac events.<sup>32,33</sup> Preclinical studies targeting circulating ceramides pharmacologically with statin therapy showed decreased serum ceramide levels and reduced rates of atheroprotection.<sup>31,34</sup> However, the contribution of ceramide dysregulation in arterial tissue remains largely unclear. The extent of our current knowledge is limited to preclinical murine models in which tissue ceramides were found to affect insulin resistance, glucose intolerance, and the accumulation of aortic atherosclerosis.<sup>35-38</sup> Mice maintained on a sphingolipid-rich diet developed larger atherosclerotic lesions,<sup>39</sup> which appeared to be more highly concentrated with low-density lipoprotein-conjugated ceramides.<sup>40</sup> Our study builds on these prior murine studies and demonstrates that in human tissue, ceramide content is significantly associated with end-stage PAD in individuals with CLTI.

Only a few studies have evaluated the effects of bioactive lipid molecules on EC viability and function.<sup>41</sup> The accumulation of arterial fatty deposits inhibits endothelial homeostasis, affects vasoactive functions in the peripheral arterial system, and reduces endothelial nitric oxide synthase. Elevated tissue ceramides can also reduce endothelial nitric oxide synthase activation and lead to impaired vasorelaxation, increased oxidative stress, and increased tissue inflammation.<sup>12,42-47</sup> Prior studies that selectively targeted ceramides demonstrated enhanced EC viability and improved arterial vasoactive function.<sup>48-52</sup> Our study similarly demonstrates that EC viability and autophagy signaling is significantly affected by C16 and that under stress conditions (with C16 supplementation), *SMPDs* play an important role in managing the excess production of ceramides from SPMs via the alternative biochemical synthesis pathway. We suspect that the observed *SMPD* downregulation in the setting of diabetes (Fig 2, G) likely represents an autogenous protective mechanism that aims to limit the overproduction of bioactive ceramides.

Our study also builds on prior findings that show that ceramide function is dependent on its lipid molecule chain length. Differences in chain lengths have a noticeable impact on the biophysical and molecular properties of ceramides, which, in turn, can affect various cellular and tissue processes.<sup>53</sup> The ceramide transport protein selectively transports C14, C16, C18, and C20 ceramides.<sup>54</sup> This selectivity in chain length affects which ceramides are more likely to traverse cell membranes and affect cellular processes. C16 ceramides can integrate into cholesterol lipid rafts, and C24 ceramides cannot.<sup>55</sup> Additionally, ceramides are highly hydrophobic molecules, which means they can bind to a wide range of



proteins, including those with critical roles in post-translational modification, cell signaling, and transcription factors responsible for gene expression.<sup>56</sup> The broad range of ceramide–protein interactions that occur in tissue might, in part, explain the variable physiologic outcomes observed in different cell types.<sup>54,56</sup> For long-chain fatty acids (ranging from C16 to C18), in particular, prior studies show that these lipid molecules play critical roles in cellular viability, apoptosis cellular machinery, and activation of protein kinases such as c-Jun N-terminal kinase and adenosine monophosphate-activated protein kinase.<sup>56</sup> Our study demonstrates that the long-chain ceramide C16 is the most abundant ceramide in diseased peripheral arterial intima. Consistent with prior studies, ceramide C16 also appears to greatly affect EC viability and function.

Ceramide biosynthesis occurs via three well-characterized biochemical pathways.<sup>25</sup> Our study findings suggest that C16 in ECs and human peripheral arterial intima is, at least in part, synthesized by SMPDs. Interestingly, SMPDs stratify as alkaline, neutral, or acidic pH catalytic enzymes and are predominantly activated under cell stress conditions and cytokine-induced tissue inflammation.<sup>57–59</sup> *SMPD1* encodes an acidic SMPD, and a deficiency in this enzyme causes Niemann-Pick disease, which is a rare fatal condition that affects lysosomal storage and lipid metabolism.<sup>60</sup> The more abundant and neutral SMPDs are expressed by *SMPD2* and *SMPD4* (on which we focused in our study; Fig 4) and appear to play vital regulatory roles in cellular proliferation machinery and apoptosis mechanisms.<sup>60–65</sup> In particular, *SMPD2* was previously linked to atheroprotection via the nitride oxide synthesis pathway and through activation of tumor necrosis factor- $\alpha$ .<sup>66,67</sup> Overall prior studies highlight the importance of SMPDs as regulatory proteins that manage cellular production of ceramides in lipid-rich environments and can ultimately affect various end organ functions.<sup>64,65</sup> Similarly, our study demonstrates that SMPDs are essential for EC proliferative activity and autophagy signaling—especially under stress conditions. In our studies, it is unclear why protective autophagy was not significantly blunted in HUVECs treated with *siGFP* control (Fig 4, B) but is likely related to the specific transfection conditions used in this experimental control. Nevertheless, we observed a consistent decrease in autophagy in all other experimental conditions (including C2 controls), demonstrating that both SMPDs and C16 affect EC viability.

Recent efforts have targeted ceramides in an attempt to reduce the risk of atheroprotection. Lipid-lowering medications such as statins and PCSK9 inhibitors are associated with a 30% reduction in circulating serum ceramides in patients with hyperlipidemia.<sup>34</sup> In preclinical murine models, selective inhibition of *CERS6*, which catalyzes the de novo biosynthesis of ceramides, demonstrated improved insulin sensitivity and reduced

dyslipidemia.<sup>67,68</sup> Interestingly, multiple Food and Drug Administration–approved drugs, mostly tricyclic antidepressants, that coincidentally inhibit SMPDs that produce ceramides via the alternative biosynthesis pathways.<sup>69</sup> Although none of these agents have been found to reduce the burden of atherosclerotic disease, several appear to improve tissue function and viability. Desipramine, an antidepressant, which reduces ceramide content in cardiomyocytes, also improved cellular viability and cardiac function and contractility.<sup>70–73</sup> Stimulation of ceramide degradation pathways has also demonstrated potential therapeutic benefits by improving insulin sensitivity and signaling.<sup>74</sup> Our study observed increased *SMPD* expression in human tibial arterial intima and that selective knockdown of *SMPD2* and *SMPD4* isoforms improved EC autophagy and proliferation in nonstress conditions (in the absence of C16 supplementation). These studies provide a new framework for ceramide targeting and provide for further exploration of ceramide and SMPD signaling in the peripheral arterial tissue of individuals at risk of PAD progression.

**Study limitations.** We acknowledge that our study has some limitations. First, despite careful tissue sampling, preparation, and dissection, the proximity of maximally and minimally diseased tibial arterial tissues could lead to sampling error and an unconscious selection bias and type II error. Nevertheless, we intentionally used our previously reported techniques, which we observed to provide robust and consistent results in elucidating differences in lipid metabolism in peripheral arterial tissue.<sup>1,21,75</sup> Second, our human cohort might not fully account for the chronic progression of disease and the range of medical comorbidities that typically afflict patients with PAD. Our clinical samples were obtained at a single point during limb amputation, which certainly narrows the perspective of our biochemical analysis and is not fully reflective of the chronic PAD disease process. Because it is not possible to obtain arterial samples from patients with PAD over time in a longitudinal fashion, we anticipate that future rodent models, or even large animal models, that are prone to atherosclerosis might help resolve this persistent limitation in investigations of PAD progression. Third, CLTI provides unique opportunities for investigating molecular mechanisms that affect atheroprotection; however, arterial samples obtained from patients afflicted by this mostly represent an end-stage disease state. In this context, our study demonstrates clear differences in ceramide content between maximally and minimally diseased peripheral arterial intima and notable correlations between ceramides and SPMs. We anticipate that future studies can further investigate whether similar mechanisms occur during earlier stages of PAD and determine how medical comorbidities (eg, chronic kidney disease, smoking habits) and critical

patient demographics such as age, sex, and systemic metabolites can affect PAD progression. Finally, although our study focused primarily on evaluating the effects of C16 on ECs, it is likely that C16 can also affect vascular smooth muscle cells in the arterial media. Future studies evaluating the ceramide-mediated autocrine and paracrine EC–vascular smooth muscle cells interactions could be a ripe area of future investigation, given the findings of our study.

## CONCLUSIONS

We report that C16 appears to be the single most elevated lipid in the tibial arterial intima of patients with CLTI. In addition, we demonstrated that excessive levels of C16 are deleterious for EC viability and homeostasis. In contrast, inhibition of ceramide production by selective knockdown of specific *SMPDs* appears to preserve EC proliferation, even under stress conditions. Our study provides the impetus for future studies to explore the role of targeting C16 and *SMPDs* as opportunities to circumvent PAD progression and the risk of limb loss associated with CLTI.

The authors thank Mrs. Batool Arif for generous technical assistance and general laboratory supervision, Theresa Belgeri for administrative support, and the Washington University Vascular Biobank Team, Mrs. Amanda Penrose, Mrs. Ashley Cosentino, and Mr. Connor Engel for specimen procurement. The authors also thank Dr. Xiaochao Wei and Dr. Xiaohua Jin for their critical suggestions and critiques. Primary data are available on reasonable request to the corresponding author.

## AUTHOR CONTRIBUTIONS

Conception and design: CS, MZ

Analysis and interpretation: YC, NH, CL, SH, FH, CS, MZ

Data collection: RM, YC, NH, CL, SH, FH

Writing the article: RM, NH, MZ

Critical revision of the article: CS, MZ

Final approval of the article: RM, YC, NH, CL, SH, FH, CS, MZ

Statistical analysis: RM, YC, NH

Obtained funding: CS, MZ

Overall responsibility: MZ

## DISCLOSURES

None.

## REFERENCES

- Zayed MA, Hsu FF, Patterson BW, et al. Diabetes adversely affects phospholipid profiles in human carotid artery endarterectomy plaques. *J Lipid Res*. 2018;59:730–738.
- White JV, Conte M, Bradbury A, et al. Building a global alliance in vascular surgery. *J Vasc Surg*. 2019;70:663–664.
- Tay S, De Silva GS, Engel CM, et al. Prevalence of elevated serum fatty acid synthase in chronic limb-threatening ischemia. *Sci Rep*. 2021;11:1–9.
- Nehler MR, Duval S, Diao L, et al. Epidemiology of peripheral arterial disease and critical limb ischemia in an insured national population. *J Vasc Surg*. 2014;60:686–695.e2.
- Fowkes FGR, Rudan D, Rudan I, et al. Comparison of global estimates of prevalence and risk factors for peripheral artery disease in 2000 and 2010: a systematic review and analysis. *Lancet*. 2013;382:1329–1340.
- Dua A, Desai SS, Patel B, et al. Preventable complications driving rising costs in management of patients with critical limb ischemia. *Ann Vasc Surg*. 2016;33:144–148.
- Hirsch AT, Hartman L, Town RJ, Virnig BA. National health care costs of peripheral arterial disease in the Medicare population. *Vasc Med*. 2008;13:209–215.
- Martinez RA, Shnayder M, Parreco J, et al. Nationally representative readmission factors in patients with claudication and critical limb ischemia. *Ann Vasc Surg*. 2018;52:96–107.
- Inzitari D, Eliasziw M, Gates P, et al. The causes and risk of stroke in patients with asymptomatic internal-carotid-artery stenosis. *N Engl J Med*. 2000;342:1693–1701.
- Linton MRF, Yancey PC, Davies SS, et al. The role of lipids and lipoproteins in atherosclerosis. In: Feingold KR, Anawalt B, Blackman MR, et al., eds. *Endotext*. MDTText.com, Inc.; South Dartmouth, MA; 2000. Accessed November 28, 2023. Available at: <https://www.ncbi.nlm.nih.gov/books/NBK343489/>.
- Hazarika S, Annex BH. Biomarkers and genetics in peripheral artery disease. *Clin Chem*. 2017;63:236–244.
- Cogolludo A, Villamor E, Perez-Vizcaino F, Moreno L. Ceramide and regulation of vascular tone. *Int J Mol Sci*. 2019;20:1–23.
- Van Brocklyn JR, Williams JB. The control of the balance between ceramide and sphingosine-1-phosphate by sphingosine kinase: oxidative stress and the seesaw of cell survival and death. *Comp Biochem Physiol B Biochem Mol Biol*. 2012;163:26–36.
- Meeusen JW, Donato LJ, Bryant SC, Baudhuin LM, Berger PB, Jaffe AS. Plasma ceramides a novel predictor of major adverse cardiovascular events after coronary angiography. *Arterioscler Thromb Vasc Biol*. 2018;38:1933–1939.
- Li PL, Gulbins E. Bioactive lipids and redox signaling: molecular mechanism and disease pathogenesis. *Antioxidants Redox Signal*. 2018;28:911–915.
- Wang DD, Toledo E, Hruby A, et al. Plasma Ceramides, Mediterranean Diet, and Incident Cardiovascular Disease in the PREDIMED Trial (Prevención con Dieta Mediterránea). *Circulation*. 2017;135:2028–2040.
- Field BC, Gordillo R, Scherer PE. The role of ceramides in diabetes and cardiovascular disease regulation of ceramides by adipokines. *Front Endocrinol*. 2020;11:1–14.
- Bismuth J, Lin P, Yao Q. Ceramide CC. A common pathway for atherosclerosis? *Atherosclerosis*. 2008;196:497–504.
- Li W, Yang X, Xing S, et al. Endogenous ceramide contributes to the transcytosis of oxLDL across endothelial cells and promotes its sub-endothelial retention in vascular wall. *Oxid Med Cell Longev*. 2014;2014:27855–27862.
- Zayed MA, Jin X, Yang C, et al. CEPT1-Mediated phospholipogenesis regulates endothelial cell function and ischemia-induced angiogenesis through PPAR $\alpha$ . *Diabetes*. 2021;70:549–561.
- Livak KJ, Schmittgen TD. Analysis of relative gene expression data using real-time quantitative PCR and the 2- $\Delta\Delta$ CT method. *Methods*. 2001;25:402–408.
- Zayed MA, Yuan W, Leisner TM, et al. CIB1 regulates endothelial cells and ischemia-induced pathological and adaptive angiogenesis. *Circ Res*. 2007;101:1185–1193.
- Zayed MA, Wei X, Park KM, et al. N-acetylcysteine accelerates amputation stump healing in the setting of diabetes. *FASEB J*. 2017;31:2686–2695.
- Davignon J, Ganz P. Role of endothelial dysfunction in atherosclerosis. *Circulation*. 2004;109:1127–1132.
- Choezom D, Gross JC. Neutral sphingomyelinase 1 regulates cellular fitness at the level of ER stress and cell cycle. bioRxiv; 2022.
- Krut O, Wiegmann K, Kashkar H, Yazdanpanah B, Krönke M. Novel tumor necrosis factor-responsive mammalian neutral sphingomyelinase-3 is a C-tail-anchored protein. *J Biol Chem*. 2006;281:13784–13793.
- Miller NE. Associations of high-density lipoprotein subclasses and apolipoproteins with ischemic heart disease and coronary atherosclerosis. *Am Heart J*. 1987;113:589–597.
- Lüscher TF, Barton M. Biology of the endothelium. *Clin Cardiol*. 1997;20:113–110.

30. Zhang DX, Zou AP, Ian LP. Ceramide-induced activation of NADPH oxidase and endothelial dysfunction in small coronary arteries. *Am J Physiol - Hear Circ Physiol*. 2003;284:H605–H612.
31. Choi RH, Tatum SM, Symons JD, Summers SA, Holland WL. Ceramides and other sphingolipids as drivers of cardiovascular disease. *Nat Rev Cardiol*. 2021;18:701–711.
32. Anroedh S, Hilvo M, Martijn Akkerhuis K, et al. Plasma concentrations of molecular lipid species predict long-term clinical outcome in coronary artery disease patients. *J Lipid Res*. 2018;59:1729–1737.
33. Jiang XC, Paultre F, Pearson TA, et al. Plasma sphingomyelin level as a risk factor for coronary artery disease. *Arterioscler Thromb Vasc Biol*. 2000;20:2614–2618.
34. Tarasov K, Ekroos K, Suoniemi M, et al. Molecular lipids identify cardiovascular risk and are efficiently lowered by simvastatin and PCSK9 deficiency. *J Clin Endocrinol Metab*. 2014;99:E45–52.
35. Park TS, Panek RL, Rekhter MD, et al. Modulation of lipoprotein metabolism by inhibition of sphingomyelin synthesis in ApoE knockout mice. *Atherosclerosis*. 2006;189:264–272.
36. Glaros EN, Kim WS, Wu BJ, et al. Inhibition of atherosclerosis by the serine palmitoyl transferase inhibitor myriocin is associated with reduced plasma glycosphingolipid concentration. *Biochem Pharmacol*. 2007;73:1340–1346.
37. Holland WL, Brozinick JT, Wang LP, et al. Inhibition of ceramide synthesis ameliorates glucocorticoid-, saturated-fat-, and obesity-induced insulin resistance. *Cell Metab*. 2007;5:167–179.
38. Hojjati MR, Li Z, Zhou H, et al. Effect of myriocin on plasma sphingolipid metabolism and atherosclerosis in apoE-deficient mice. *J Biol Chem*. 2005;280:10284–10289.
39. Li Z, Basterr MJ, Hailemariam TK, et al. The effect of dietary sphingolipids on plasma sphingomyelin metabolism and atherosclerosis. *Biochim Biophys Acta - Mol Cell Biol Lipids*. 2005;1735:130–134.
40. Schissel SL, Tweedie-Hardman J, Rapp JH, Graham C, Williams KJ, Tabas I. Rabbit aorta and human atherosclerotic lesions hydrolyze the sphingomyelin of retained low-density lipoprotein. Proposed role for arterial-wall sphingomyelinase in subendothelial retention and aggregation of atherogenic lipoproteins. *J Clin Invest*. 1996;98:1455–1464.
41. Levade T, Malagarie-Cazenave S, Gouazé V, et al. Ceramide in apoptosis: a revisited role. *Neurochem Res*. 2002;27:601–607.
42. Li H, Junk P, Huwiler A, et al. Dual effect of ceramide on human endothelial cells: Induction of oxidative stress and transcriptional upregulation of endothelial nitric oxide synthase. *Circulation*. 2002;106:2250–2256.
43. Mogami K, Kishi H, Kobayashi S. Sphingomyelinase causes endothelium-dependent vasorelaxation through endothelial nitric oxide production without cytosolic Ca<sup>2+</sup> elevation. *FEBS Lett*. 2005;579:393–397.
44. Johns DC, Jin JS, Wilde DW, Webb RC. Ceramide-induced vasorelaxation: an inhibitory action on protein kinase C. *Gen Pharmacol*. 1999;33:415–421.
45. Moral-Sanz J, Gonzalez T, Menendez C, et al. Ceramide inhibits Kv currents and contributes to TP-receptor-induced vasoconstriction in rat and human pulmonary arteries. *Am J Physiol Cell Physiol*. 2011;301:186–194.
46. Sanvicens N, Cotter TG. Ceramide is the key mediator of oxidative stress-induced apoptosis in retinal photoreceptor cells. *J Neurochem*. 2006;98:1432–1444.
47. Gomez-Muñoz A, Presa N, Gomez-Larrauri A, Rivera IG, Trueba M, Ordoñez M. Control of inflammatory responses by ceramide, sphingosine 1-phosphate and ceramide 1-phosphate. *Prog Lipid Res*. 2016;61:51–62.
48. Zhang QJ, Holland WL, Wilson L, et al. Ceramide mediates vascular dysfunction in diet-induced obesity by PP2A-mediated dephosphorylation of the eNOS-Akt complex. *Diabetes*. 2012;61:1848–1859.
49. Dobrowsky RT, Kamibayashi C, Mumby MC, Hannun YA. Ceramide activates heterotrimeric protein phosphatase 2A. *J Biol Chem*. 1993;268:15523–15530.
50. Kudo N, Kumagai K, Tomishige N, et al. Structural basis for specific lipid recognition by CERT responsible for nonvesicular trafficking of ceramide. *Proc Natl Acad Sci U S A*. 2008;105:488–493.
51. Thomas RL, Matsko CM, Lotze MT, Amoscato AA. Mass spectrometric identification of increased C16 ceramide levels during apoptosis. *J Biol Chem*. 1999;274:30580–30588.
52. Obeid LM, Linardic CM, Karolak LA, Hannun YA. Programmed cell death induced by ceramide. *Science*. 1993;259:1769–1771.
53. Grösch S, Schiffmann S, Geisslinger G. Chain length-specific properties of ceramides. *Prog Lipid Res*. 2012;51:50–62.
54. Kumagai K, Yasuda S, Okemoto K, Nishijima M, Kobayashi S, Hanada K. CERT mediates intermembrane transfer of various molecular species of ceramides. *J Biol Chem*. 2005;280:6488–6495.
55. ten Grotenhuis E, Demel RA, Ponec M, Boer DR, van Miltenburg JC, Bouwstra JA. Phase behavior of stratum corneum lipids in mixed Langmuir-Blodgett monolayers. *Biophys J*. 1996;71:1389–1399.
56. Watanabe T, Ninomiya H, Saitou T, et al. Therapeutic effects of the PKR inhibitor C16 suppressing tumor proliferation and angiogenesis in hepatocellular carcinoma in vitro and in vivo. *Sci Rep*. 2020;10:5133.
57. GATT S. Enzymic hydrolysis and synthesis OF ceramides. *J Biol Chem*. 1963;238:3131–3133.
58. Hannun YA. Functions of ceramide in coordinating cellular responses to stress. *Science*. 1996;274:1855–1859.
59. Sathishkumar K, Gao X, Raghavamenon AC, Murthy SN, Kadowitz PJ, Uppu RM. *Free Radicals and Antioxidant Protocols*. 2010;610:51–61.
60. Marathe S, Schissel SL, Yellin MJ, et al. Human vascular endothelial cells are a rich and regulatable source of secretory sphingomyelinase. Implications for early atherogenesis and ceramide-mediated cell signaling. *J Biol Chem*. 1998;273:4081–4088.
61. Schulze PC, Drosatos K, Goldberg IJ. Lipid use and misuse by the heart. *Circ Res*. 2016;118:1736–1751.
62. Marchesini N, Osta W, Bielawski J, Luberto C, Obeid LM, Hannun YA. Role for mammalian neutral sphingomyelinase 2 in confluence-induced growth arrest of MCF7 cells. *J Biol Chem*. 2004;279:25101–25111.
63. Karakashian AA, Giltiy NV, Smith GM, Nikolova-Karakashian MN. Expression of neutral sphingomyelinase-2 (NSMase-2) in primary rat hepatocytes modulates IL-beta-induced JNK activation. *FASEB J Off Publ Fed Am Soc Exp Biol*. 2004;18:968–970.
64. Marchesini N, Luberto C, Hannun YA. Biochemical properties of mammalian neutral sphingomyelinase2 and its role in sphingolipid metabolism. *J Biol Chem*. 2003;278:13775–13783.
65. Tomiuk S, Hofmann K, Nix M, Zumbansen M, Stoffel W. Cloned mammalian neutral sphingomyelinase: functions in sphingolipid signaling. *Proc Natl Acad Sci U S A*. 1998;95:3638–3643.
66. Palma CD, Meacci E, Perrotta C, Bruni P, Clementi E. Endothelial nitric oxide synthase activation by tumor necrosis factor  $\alpha$  through neutral sphingomyelinase 2, sphingosine kinase 1, and sphingosine 1 phosphate receptors. *Arterioscler Thromb Vasc Biol*. 2006;26:99–105.
67. Hammerschmidt P, Ostkotte D, Nolte H, et al. CerS6-Derived sphingolipids Interact with mff and promote mitochondrial fragmentation in obesity. *Cell*. 2019;177:1536–1552.e23.
68. Lin CH, Lee SY, Zhang CC, et al. Fenretinide inhibits macrophage inflammatory mediators and controls hypertension in spontaneously hypertensive rats via the peroxisome proliferator-activated receptor gamma pathway. *Drug Des Devel Ther*. 2016;10:3591–3597.
69. Kornhuber J, Muehlbacher M, Trapp S, et al. Identification of novel functional inhibitors of acid sphingomyelinase. *PLoS One*. 2011;6:1–13.
70. Chung HY, Kollmeyer AS, Schrepper A, et al. Adjustment of dysregulated ceramide metabolism in a murine model of sepsis-induced cardiac dysfunction. *Int J Mol Sci*. 2017;18:839.
71. Kornhuber J, Hoertel N, Gulbins E. The acid sphingomyelinase/ceramide system in COVID-19. *Mol Psychiatry*. 2022;27:307–314.
72. Adada M, Luberto C, Canals D. Inhibitors of the sphingomyelin cycle: sphingomyelin synthases and sphingomyelinases. *Chem Phys Lipids*. 2016;197:45–59.
73. Yu Z, Peng Q, Huang Y. Potential therapeutic targets for atherosclerosis in sphingolipid metabolism. *Clin Sci*. 2019;133:763–776.
74. Chavez JA, Holland WL, Bär J, Sandhoff K, Summers SA. Acid ceramidase overexpression prevents the inhibitory effects of saturated fatty acids on insulin signaling. *J Biol Chem*. 2005;280:20148–20153.
75. Engel C, Meade R, Harroun N, et al. Altered peroxisome proliferator-activated receptor alpha signaling in variably diseased peripheral arterial segments. *Front Cardiovasc Med*. 2022;9:1–13.